Photophysics

International Edition: DOI: 10.1002/anie.201504588
German Edition: DOI: 10.1002/ange.201504588

Excited-State Dynamic Planarization of Cyclic Oligothiophenes in the Vicinity of a Ring-to-Linear Excitonic Behavioral Turning Point

Kyu Hyung Park, Pyosang Kim, Woojae Kim, Hideyuki Shimizu, Minwoo Han, Eunji Sim, Masahiko Iyoda,* and Dongho Kim**

Abstract: *Excited-state dynamic planarization processes play a crucial role in determining exciton size in cyclic systems, as reported for π-conjugated linear oligomers. Herein, we report time-resolved fluorescence spectra and molecular dynamics simulations of π-conjugated cyclic oligothiophenes in which the number of subunits was chosen to show the size-dependent dynamic planarization in the vicinity of a ring-to-linear behavioral turning point. Analyses on the evolution of the total fluorescence intensity and the ratio between 0–1 to 0–0 vibronic bands suggest that excitons formed in a cyclic oligothiophene composed of six subunits fully delocalize over the cyclic carbon backbone, whereas those formed in larger systems fail to achieve complete delocalization. With the aid of molecular dynamics simulations, it is shown that distorted structures unfavorable for efficient exciton delocalization are more easily populated as the size of the cyclic system increases.*

A wide range of π-conjugated oligomers and polymers have been developed as a result of their promising applicability in various optoelectronic devices.[1–5] In such systems, the extent of exciton delocalization plays a crucial role in determining the device performance.[5–7] A number of experimental and theoretical works have revealed the two key processes governing exciton size: exciton self-trapping induced by the C=C stretching motion and exciton delocalization induced by dynamic planarization.[8–15] Exciton self-trapping occurs on a timescale of less than 100 fs and causes the exciton to localize in the conjugative segments defined primarily by torsions and kinks within the Franck–Condon state geometry.[8–11] On the other hand, exciton delocalization occurs on a picosecond timescale and has a contrasting effect on exciton size as it decreases inter-ring torsional angles and thereby enhances π-orbital overlap between chromophoric units. As a consequence of dynamic planarization, the quinoidal character of the system becomes manifest and as a result confined excitons delocalize over the carbon backbone.[12–15]

Many researchers have examined the effect of excited-state structural rearrangement on the extent of exciton delocalization. By varying lengths of linear oligomers, they found that the exciton wavefunction vanishes on the periphery of a carbon chain, which is often referred as the chain-end effect.[8,16,17] Furthermore, it was shown that the linear geometry is prone to conformational disorder, which disrupts π conjugation and hampers exciton delocalization.[18–21] In contrast, cyclic oligomers, such as cycloparaphenylenes (CPPs),[22–25] cyclothiophenes,[26–28] and porphyrin nanorings,[29–31] have drawn considerable attention in recent years as they were predicted to exhibit less, or no, chain-end effect.[23,27,29,32] However, continued studies have collectively demonstrated that the common characteristics of a cyclic system can be lost depending on the size of the system. For example, Aggarwal et al. have recently shown that the excitons formed in large π-conjugated macrocycles composed of six phenylcarbazole-based units localize to dimer-length segments of random orientation.[33] In CPPs, Adamska et al. have shown that excitons localized to form distorted structures in large CPPs, whereas uniform cyclic structures are maintained in small CPPs as a result of complete delocalization of excitons.[34] Parkinson et al. studied the difference in the size of the absorbing and emitting states of porphyrin nanorings and demonstrated that exciton localization in large porphyrin nanorings results in a loss of ring-like behaviors.[35] In line with previous studies, our group recently published a comparative study on the exciton delocalization process of linear and cyclic oligothiophenes.[36] By analyzing the evolution of transient fluorescence spectra, we suggested that the conformational disorder is significantly decreased by forming a cyclic geometry. In a cyclic oligothiophene composed of ten thiophene units (**C-10T$_{2V}$**), a dynamic planarization process allows complete delocalization of the exciton over the cyclic framework (herein termed formation of a cyclic exciton), whereas in larger rings (from **C-15T$_{3V}$** to **C-30T$_{6V}$**), the same process fails to produce circular excitons. A consecutive study on **C-10T$_{2V}$** by single-molecule spectroscopy has differentiated the spectral features originating from torsional defects and small torsional disorder, which led to the conclusion that the ensemble of **C-10T$_{2V}$** contains an appreciable portion of excitons which cannot completely delocalize over the cyclic framework (herein termed acyclic excitons).[37]

According to previous studies, excitons that form in π-conjugated cyclic oligomers undergo complex evolution

[*] K. H. Park, Dr. P. Kim, W. Kim, Prof. Dr. D. Kim
Department of Chemistry and Spectroscopy Laboratory for Functional π-Electronic Systems, Yonsei University
Seoul 120-749 (Korea)
E-mail: dongho@yonsei.ac.kr
Dr. H. Shimizu, Prof. Dr. M. Iyoda
Department of Chemistry
Graduate School of Science and Engineering
Tokyo Metropolitan University, Tokyo 192-0397 (Japan)
E-mail: iyoda@tmu.ac.jp
Dr. M. Han, Prof. Dr. E. Sim
Department of Chemistry and Institute of Nano-Bio Molecular Assemblies, Yonsei University, Seoul 120-749 (Korea)
E-mail: esim@yonsei.ac.kr

Supporting information for this article is available on the WWW under http://dx.doi.org/10.1002/anie.201504588.

depending on the size of the system. The ring-size dependence of the primary process, that is, exciton self-trapping, has been systematically studied in a number of systems. However, the effect of dynamic planarization on the exciton size in cyclic systems has not been thoroughly investigated. In this regard, we prepared a set of macrocyclic oligothiophenes (Figure 1) in which the number of thiophene units was selected to examine the dynamic planarization process near the turning point of ring-to-linear exciton behavior.

The steady-state absorption and fluorescence spectra of cyclic oligothiophenes in toluene are shown in Figure 2 and their photophysical parameters are tabulated in Table S1 in Supporting Information. The absorption spectrum of **C-6T** has characteristics similar to other small cyclic systems previously reported, such as cyclothiophenes composed of eight units[27] or CPPs composed of less than nine units.[24,25] In these fully conjugated, flat, cyclic oligomers, energy states are arranged to produce a forbidden S_0–S_1 transition and doubly degenerate S_0–S_2, S_0–S_3 transitions.[38,39] In this sense, the sharp absorption band of **C-6T** at $\lambda = 412$ nm corresponds to the allowed degenerate transitions and the long tail stretched down to $\lambda = 550$ nm corresponds to the forbidden lowest energy transition, which, presumably, gains oscillator strength by Herzberg–Teller intensity borrowing.[40] In going from **C-6T** to **C-12T** the lowest energy absorptions become gradually more intense. This change can be attributed to the lifting of cyclic symmetry by conformational disorder which redistributes the oscillator strength from pairwise degenerate transitions to the forbidden lowest-energy transition. Thus, the gradual increase in intensity of the lowest-energy transition reflects the increasing conformational disorder with an increase in the size of the cyclic oligothiophenes.

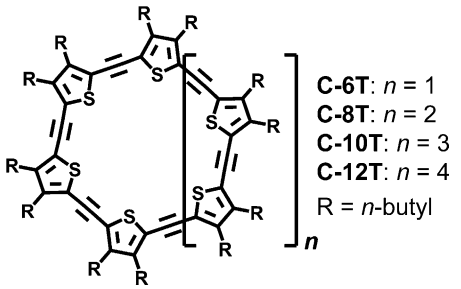

Figure 1. Molecular structures of cyclic oligothiophenes.

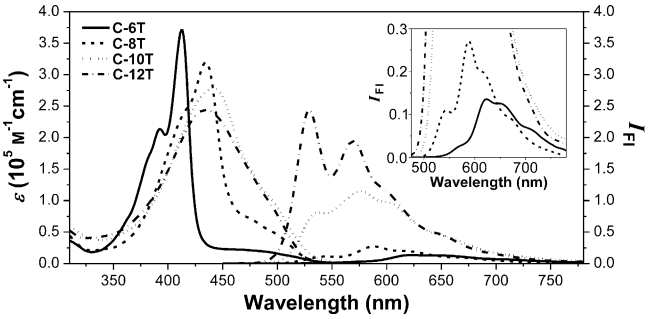

Figure 2. Steady-state UV/Vis absorption (left) and fluorescence spectra (right) of cyclic oligothiophenes in toluene. The samples were excited at the wavelength of their absorption maxima. The fluorescence intensities (I_{fl}) are scaled to reflect their fluorescence quantum yields. Inset: Steady-state fluorescence spectra of **C-6T** and **C-8T**.

As suggested in previous studies, the steady-state fluorescence of cyclic oligothiophenes is a consequence of structural relaxation processes along steep excited-state potential.[36] In this sense, the lack of mirror-image symmetry in **C-12T**, which is often observed in typical π-conjugated linear oligomers, signifies large excited-state structural rearrangement along the torsional coordinate. It is worth noting that the 0–0 to 0–1 vibronic band ratio for the steady-state fluorescence spectrum of **C-12T** is also similar to that of P3HT (poly(3-hexylthiophene)).[41] The theoretical work done by Hestand and Spano suggests that in an ideal cyclic conjugated polymer, the fully delocalized exciton (cyclic exciton) can be characterized by a complete suppression of the 0–0 vibronic band.[42] Structural or thermal disorder disrupting exciton coherence allows the 0–0 vibronic band to become more intense. This result is coincident with the Herzberg–Teller intensity borrowing described by Yong et al., which assigns the 0–0 vibronic transition to a forbidden transition and attributes the presence of 0–1 or higher-order vibronic bands to dynamic distortion involving non-totally symmetric modes.[43] In Figure 2, it is easy to notice that the 0–1 to 0–0 vibronic band intensity ratio (I^{0-1}/I^{0-0}) decreases with increasing the size of the molecule. This trend suggests that the cyclic oligothiophenes in their excited states are conformationally disordered, where the disorder increases with increasing the size of the system. This speculation is further supported by the trends in fluorescence quantum yields and radiative rate constants (Table S1).[43] As the radiative rate constant k_r is proportional to the oscillator strength of an emissive state,[44] an increase in k_r value with increasing the size of the molecule can be related to the size-dependent conformational disorder, which leads to a lowering of the symmetry and an increase of the oscillator strength in the emissive state.

To investigate the development of excited-state conformational disorder as a function of time, we employed femtosecond fluorescence upconversion technique. Figure 3a–d shows the time-resolved fluorescence spectra (TRFS) for compounds **C-6T**, **C-8T**, **C-10T**, and **C-12T**. The spectra were reconstructed from the fluorescence decay profiles analyzed by global fitting using two time variables (τ_1 and τ_2) and one constant (τ_{fl}) fixed to the fluorescence lifetimes obtained from time-correlated single photon counting (TCSPC) measurements (Table S4).[12] The two time variables were used to fit the complex spectral evolution induced by the dynamic planarization process.[15] Notice that the spectral shift, indicative of exciton delocalization, is clear in **C-10T** and **C-12T**, whereas in **C-6T** and **C-8T** such behavior is less appreciable, implying a stagnant exciton size for the two planar systems. Instead, a fast decrease in intensity with changes in the vibronic band ratio is recognized. To perform detailed analyses on the dynamic planarization reflected in the spectral evolution, the TRFS were fitted with a sum of two to three Gaussian functions.[45]

Figure 3e shows the plot of the normalized total fluorescence intensity as a function of time. The rapid suppression of fluorescence intensity does not seem to originate from the population decay of a singlet excited state, but is due to

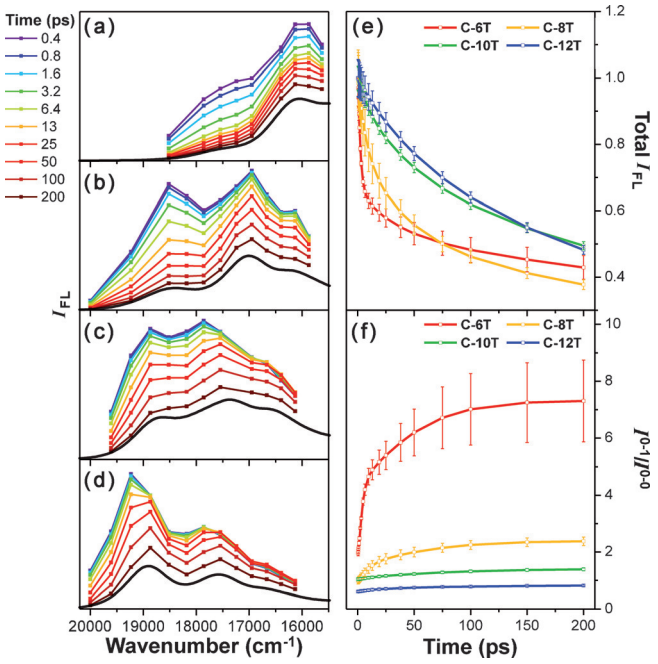

Figure 3. Reconstructed TRFS of a) **C-6T**, b) **C-8T**, c) **C-10T**, and d) **C-12T** in toluene. e) Total fluorescence intensity (total I_{fl}) and f) ratio of the spectrally integrated fluorescence intensity of the 0–1 to 0–0 vibronic bands (I^{0-1}/I^{0-0}) calculated from TRFS. All samples were excited at $\lambda = 400$ nm.

a symmetry-induced decrease of the oscillator strength of an emitting state. This occurs through the dynamic planarization of distorted cyclic carbon backbones imposing a cyclic symmetry constraint on the partially allowed S_1 state.[36] Thus, the two fast lifetimes in the total fluorescence intensity decays are attributed to a dynamic planarization process. The sum of two amplitudes (A_{dp}) and the amplitude-weighted average lifetimes of dynamic planarization (τ_{dp}) are tabulated in Table 1. With increasing the size of the molecule, the time constants for dynamic planarization increases from 11 to 66 ps and its contribution to the total fluorescence decay decreases from 47.3 to 29.5 %. This trend suggests that the dynamics and the extent of cyclic symmetry recovery are determined by the interplay of innate structural flexibility and the quinoidal character in the excited state. Although dynamic planarization stabilizes the quinoidal bonding character in the excited state by decreasing inter-ring torsional angles, thermal perturbation acts as an opposing force which hinders the system from reaching an ideal cyclic conformation. The degree of cyclic symmetry recovery is limited to an equilibrium in which the two counteracting effects are in balance. As the decreasing contribution of dynamic planarization implies, the equilibrium is biased to distorted conformations as the size of the ring increases.

Table 1: Summary of the parameters for the total intensity decay and the ratio between 0–1 and 0–0 vibronic bands.

Sample	τ_{dp}[a] [ps]	τ_{fl} [ps]	A_{dp}[b] [%]	A_{fl} [%]	$(I^{0-1}/I^{0-0})_i$[c]	$(I^{0-1}/I^{0-0})_f$[d]
C-6T	11	970	47.3	52.7	1.96	7.31
C-8T	26	640	48.8	51.2	0.98	2.38
C-10T	49	620	33.4	66.6	1.04	1.39
C-12T	66	480	29.5	70.5	0.60	0.81

[a] Amplitude-weighted average lifetime. [b] Amplitude sum of dynamic planarization. [c] Initial and [d] final 0–1 to 0–0 vibronic band ratio.

Figure 3 f shows the evolution of the intensity ratio between the 0–0 and 0–1 vibronic bands (I^{0-1}/I^{0-0}) as a function of time. Again, for all cyclic oligothiophenes, the ratios rapidly increase on the timescale of dynamic planarization. In conjunction with the rapid fluorescence suppression, the rise in I^{0-1}/I^{0-0} values is also a result of exciton delocalization aided by dynamic planarization. Based on the previous interpretations by Hestand and Spano[42] and Yong et al,[43] the high initial I^{0-1}/I^{0-0} value in the case of **C-6T** indicates that the dynamic planarization of this molecule starts from a relatively planar molecular geometry, which approaches a nearly ideal cyclic geometry by removal of the marginal disorder present in the starting molecular configuration. In the case of **C-12T**, the low initial I^{0-1}/I^{0-0} value, which is similar to those of typical linear π-conjugated oligomers, suggests that the starting shape of the exciton is linear. Although dynamic planarization in **C-12T** extends the exciton size, severe torsional disorder induced by thermal perturbation impedes full-ring exciton delocalization.[15] Thus, the final I^{0-1}/I^{0-0} value of **C-12T** implies that excitons cannot fully delocalize within the structure (acyclic exciton). Similarly, we can conclude that exciton formed in **C-10T** starts from and ends with an acyclic geometry but its curvature is indicated by a larger I^{0-1}/I^{0-0} value than that of **C-12T**.[42] A further increase is detected in **C-8T** which can be interpreted by the formation of a near-cyclic exciton and, finally, the large I^{0-1}/I^{0-0} value in the case of **C-6T** is assigned to the realization of a fully cyclic exciton, that is, excitons can fully delocalize over the cyclic molecular backbone.

Size-dependent conformational disorder is further supported by the existence of various conformers obtained from molecular dynamics (MD) simulations performed with the NAMD program.[46] We obtained 10000 different molecular conformations from 5 ns of simulation, from which mean planes of backbone atoms and inter-thiophene torsional angles were calculated (see the Supporting Information for details).

To evaluate the planarity of the cyclic backbone, we introduce a model parameter D which is the sum of the squares of the distances from a mean plane normalized by the number of constituent thiophene units. Figure 4 a shows the distribution of parameter D for the simulated conformers. **C-6T** shows surprisingly sharp distribution near 0 Å^2 whereas **C-12T** shows a broad dragging distribution to 50 Å^2 (distribution over 30 Å^2 is truncated as a result of low counts). The narrow distribution of **C-6T** and **C-8T** approaching 0 Å^2 is a result of large ring strain, whereas broad distribution of **C-10T** and **C-12T** is a result of structures without strain. It is easy to expect that chain bending and folding cost a large amount of energy for systems with large strain, whereas thermal energy at room temperature is enough to form nonplanar structures for systems with little strain.[47] This presumption is supported by the shape of the distributions resembling that of a Maxwell–Boltzmann distribution, which describes the distribution of the population over quantized energy states in thermal equilibrium. Thus, in the presence of

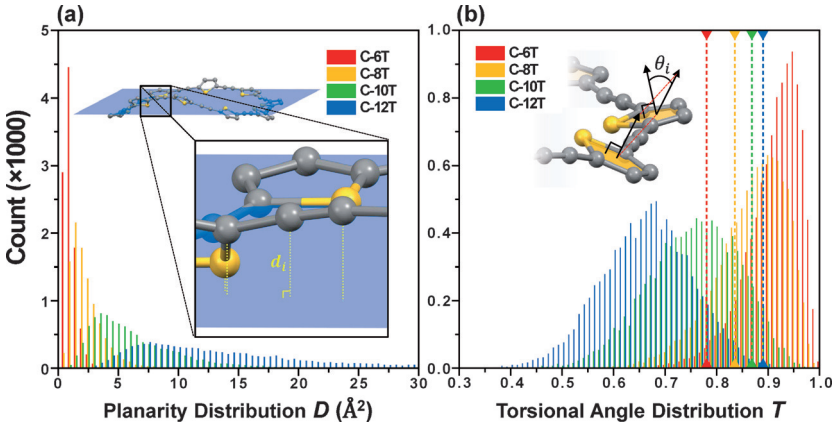

Figure 4. Distribution of a) the planarity parameter *D* and b) the torsional angle parameter *T*, calculated from 10000 conformations generated by MD simulations. The vertical dashed lines in (b) indicates the cyclic π-electron delocalization boundary values of **C-6T** (red), **C-8T** (yellow), **C-10T** (green), and **C-12T** (blue). Further details provided in the text and the Supporting Information.

identical thermal perturbation, **C-6T** and **C-8T** retain relatively planar geometries favorable for π-electron delocalization, whereas **C-10T** and **C-12T** fail to preserve planar geometry and, thus, acyclic excitons are likely to form.

As torsional potentials of π-conjugated systems are often modelled with sinusoidal functions,[48,49] we introduce another model parameter *T* for torsional angle distribution. *T* is the sum of all absolute cosine values of dihedral angles between two neighboring thiophene units which is normalized by the number of thiophene units in a system. $T=1$ represents a planar disorder-free conformation and $T=0$ represents a complete loss of π-electron delocalization. Figure 4b shows the distribution of *T* values for all cyclic oligothiophenes. The narrow distribution near the value of 1 for **C-6T** indicates that **C-6T** has stable π-electron delocalization that stretches over the whole carbon backbone. As reflected in the shift of the maxima in going from **C-6T** to **C-12T**, increasing the number of thiophene units increases the torsional disorder and heterogeneity of the system. Introducing a conjugation cutoff angle of 70°, which has been suggested by De Leener et al.,[19] allows us to estimate the proportion of conformations which have torsional defects. Conformers with *T* values smaller than the boundary values, indicated as colored dashed lines in Figure 4b, can be considered to exhibit incomplete π-electron delocalization. In **C-6T** and **C-8T**, the major proportions (97% for **C-6T** and 69% for **C-8T**) of the distribution are positioned on the side of the *T* value larger than their boundary values, whereas in **C-10T** and **C-12T**, only small portions (8.3% for **C-10T** and 0.18% for **C-12T**) reside on the side of *T* larger than the boundary values. Although the force-field parameters we employed cannot accurately reflect the excited-state torsional potential, when combined with the size-dependent symmetry recovery and exciton delocalization demonstrated in the TRFS the simulation suggests that excitons can delocalize fully, that is, a fully cyclic exciton is formed, only in **C-6T**. Above a certain size boundary, in this case the size of **C-8T**, excitons in cyclic systems tend to localize as a result of conformational disorder which disrupts efficient π-electron delocalization.

Exciton delocalization processes by dynamic planarization are schematically presented in Figure 5 for the two extreme cases, **C-6T** and **C-12T**. The exciton size in **C-6T** does not significantly increase because of its low initial disorder and dynamic planarization aids the formation of an ideal planar cyclic geometry. On the other hand, the dynamic planarization process in **C-12T** extends the exciton size but the exciton cannot completely delocalize because of a large distortion in the carbon chain.

In summary, we have investigated the size-dependent excited-state dynamic planarization processes in cyclic oligothiophenes using a femtosecond fluorescence upconversion technique. From the abrupt total intensity decay and concurrent rise in I^{0-1}/I^{0-0} values, we found that complete cyclic delocalization of the exciton occurs for **C-6T**, whereas **C-8T** attains excitons of nearly cyclic geometry and only acyclic excitons are formed for **C-10T** and **C-12T**. MD simulations support this observation by generating conformers with stable π-electron delocalization in the case of **C-6T** and **C-8T**, whereas conformers with torsional defects are generated in the case of **C-10T** and **C-12T**. Herein, we suggest that the exciton delocalization length obtained through excited-state dynamic planarization is no longer than the size of eight thiophene units. We believe that our findings on the size-dependent exciton delocalization in π-conjugated cyclic oligothiophenes will provide essential information for designing functional materials that have cyclic geometry and in which superior delocalization of excitons is possible.

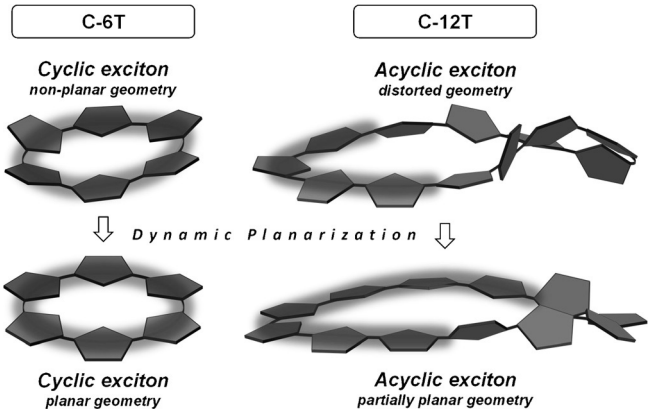

Figure 5. Schematic representation of dynamic planarization processes for cyclic oligothiophenes. In **C-6T**, excitons can fully delocalize over the cyclic molecular backbone (termed a cyclic exciton). In **C-12T**, excitons cannot achieved complete delocalization (termed an acyclic exciton) as a result of severe conformational disorder present in the system.

Acknowledgements

The work at Yonsei University was supported by Global Research Laboratory through the National Research Foundation of Korea (NRF) (2013K1A1A2A02050183) through

the National Research Foundation of Korea (NRF) funded by the Ministry of Science, ICT (Information and Communication Technologies), and Future Planning (D.K.), and by the National Research Foundation (2012R1A1A2004782; to E.S.). The work at Tokyo Metropolitan University was supported by a Grant-in-Aid for Scientific Research from JSPS and by CREST of JST (Japan Science and Technology Corporation; to M.I.).

Keywords: conformation analysis · conjugation · excitons · oligothiophenes · photophysics

How to cite: *Angew. Chem. Int. Ed.* **2015**, *54*, 12711 – 12715
Angew. Chem. **2015**, *127*, 12902 – 12906

[1] H. Sirringhaus, N. Tessler, R. H. Friend, *Science* **1998**, *280*, 1741 – 1744.
[2] A. Facchetti, *Nat. Mater.* **2013**, *12*, 598 – 600.
[3] A. J. Heeger, *Chem. Soc. Rev.* **2010**, *39*, 2354 – 2371.
[4] W. Barford in *Electronic and Optical Properties of Conjugated Polymers*, Oxford University Press, New York, UK, **2005**.
[5] M. T. Dang, L. Hirsch, G. Wantz, J. D. Wuest, *Chem. Rev.* **2013**, *113*, 3734 – 3765.
[6] A. Kohler, D. A. dos Santos, D. Beljonne, Z. Shuai, J.-L. Bredas, A. B. Holmes, A. Kraus, K. Mullen, R. H. Friend, *Nature* **1998**, *392*, 903 – 906.
[7] S. M. Falke, C. A. Rozzi, D. Brida, M. Maiuri, M. Amato, E. Sommer, A. De Sio, A. Rubio, G. Cerullo, E. Molinari, C. Lienau, *Science* **2014**, *344*, 1001 – 1005.
[8] S. Tretiak, A. Saxena, R. L. Martin, A. R. Bishop, *Phys. Rev. Lett.* **2002**, *89*, 097402.
[9] N. P. Wells, D. A. Blank, *Phys. Rev. Lett.* **2008**, *100*, 086403.
[10] W. Yu, P. J. Donohoo-Vallett, J. Zhou, A. E. Bragg, *J. Chem. Phys.* **2014**, *141*, 044201.
[11] E. Busby, E. C. Carroll, E. M. Chinn, L. Chang, A. J. Moulé, D. S. Larsen, *J. Phys. Chem. Lett.* **2011**, *2*, 2764 – 2769.
[12] N. Banerji, S. Cowan, E. Vauthey, A. J. Heeger, *J. Phys. Chem. C* **2011**, *115*, 9726 – 9739.
[13] G. Duvanel, J. Grilj, A. Schuwey, A. Gossauerb, E. Vauthey, *Photochem. Photobiol. Sci.* **2007**, *6*, 956 – 963.
[14] W. Yu, J. Zhou, A. E. Bragg, *J. Phys. Chem. Lett.* **2012**, *3*, 1321 – 1328.
[15] N. M. Albu, D. J. Yaron, *J. Phys. Chem. C* **2013**, *117*, 12299 – 12306.
[16] I. H. Nayyar, E. R. Batista, S. Tretiak, A. Saxena, D. L. Smith, R. L. Martin, *J. Phys. Chem. Lett.* **2011**, *2*, 566 – 571.
[17] S. Rodríguez González, M. C. Ruiz Delgado, R. Caballero, P. De La Cruz, F. Langa, J. T. López Navarrete, J. Casado, *J. Am. Chem. Soc.* **2012**, *134*, 5675 – 5681.
[18] T. E. Dykstra, E. Hennebicq, D. Beljonne, J. Gierschner, G. Claudio, E. R. Bittner, J. Knoester, G. D. Scholes, *J. Phys. Chem. B* **2009**, *113*, 656 – 667.
[19] C. De Leener, E. Hennebicq, J. C. Sancho-Garcia, D. Beljonne, *J. Phys. Chem. B* **2009**, *113*, 1311 – 1322.
[20] W. Barford, D. G. Lidzey, D. V. Makhov, A. J. H. Meijer, *J. Chem. Phys.* **2010**, *133*, 044504.
[21] D. Venkateshvaran, M. Nikolka, A. Sadhanala, V. Lemaur, M. Zelazny, M. Kepa, M. Hurhangee, A. J. Kronemeijer, V. Pecunia, I. Nasrallah, I. Romanov, K. Broch, I. McCulloch, D. Emin, Y. Olivier, J. Cornil, D. Beljonne, H. Sirringhaus, *Nature* **2014**, *515*, 384 – 388.
[22] R. Jasti, J. Bhattacharjee, J. B. Neaton, C. R. Bertozzi, *J. Am. Chem. Soc.* **2008**, *130*, 17646 – 17647.
[23] B. M. Wong, *J. Phys. Chem. C* **2009**, *113*, 21921 – 21927.
[24] T. Iwamoto, Y. Watanabe, Y. Sakamoto, T. Suzuki, S. Yamago, *J. Am. Chem. Soc.* **2011**, *133*, 8354 – 8361.
[25] P. J. Evans, E. R. Darzi, R. Jasti, *Nat. Chem.* **2014**, *6*, 404 – 408.
[26] F. Zhang, G. Götz, H. D. F. Winkler, C. A. Schalley, P. Bäuerle, *Angew. Chem. Int. Ed.* **2009**, *48*, 6632 – 6635; *Angew. Chem.* **2009**, *121*, 6758 – 6762.
[27] E. Mena-Osteritz, F. Zhang, G. Götz, P. Reineker, P. Bäuerle, *Beilstein J. Nanotechnol.* **2011**, *2*, 720 – 726.
[28] F. Zhang, G. Götz, E. Mena-Osteritz, M. Weil, B. Sarkar, W. Kaimc, P. Bäuerle, *Chem. Sci.* **2011**, *2*, 781 – 784.
[29] M. Hoffmann, J. Karnbratt, M. H. Chang, L. M. Herz, B. Albinsson, H. L. Anderson, *Angew. Chem. Int. Ed.* **2008**, *47*, 4993 – 4996; *Angew. Chem.* **2008**, *120*, 5071 – 5074.
[30] D. V. Kondratuk, L. M. A. Perdigao, M. C. O'Sullivan, S. Svatek, G. Smith, J. N. O'Shea, P. H. Beton, H. L. Anderson, *Angew. Chem. Int. Ed.* **2012**, *51*, 6696 – 6699; *Angew. Chem.* **2012**, *124*, 6800 – 6803.
[31] J. Q. Gong, P. Parkinson, D. V. Kondratuk, G. Gil-Ramirez, H. L. Anderson, L. M. Herz, *J. Phys. Chem. C* **2015**, *119*, 6414 – 6420.
[32] K. Nakao, M. Nishimura, T. Tamachi, Y. Kuwatani, H. Miyasaka, T. Nishinaga, M. Iyoda, *J. Am. Chem. Soc.* **2006**, *128*, 16740 – 16747.
[33] A. V. Aggarwal, A. Thiessen, A. Idelson, D. Kalle, D. Würsch, T. Stangl, F. Steiner, S. Jester, J. Vogelsang, S. Höger, J. M. Lupton, *Nat. Chem.* **2013**, *5*, 964 – 970.
[34] L. Adamska, I. Nayyar, H. Chen, A. K. Swan, N. Oldani, S. Fernandez-Alberti, M. R. Golder, R. Jasti, S. K. Doorn, S. Tretiak, *Nano Lett.* **2014**, *14*, 6539 – 6546.
[35] P. Parkinson, D. V. Kondratuk, C. Menelaou, J. Q. Gong, H. L. Anderson, L. M. Herz, *J. Phys. Chem. Lett.* **2014**, *5*, 4356 – 4361.
[36] P. Kim, K. H. Park, W. Kim, T. Tamachi, M. Iyoda, D. Kim, *J. Phys. Chem. Lett.* **2015**, *6*, 451 – 456.
[37] J. Yang, S. Ham, T. W. Kim, K. H. Park, K. Nakao, H. Shimizu, M. Iyoda, D. Kim, *J. Phys. Chem. B* **2015**, *119*, 4116 – 4126.
[38] M. Bednarz, P. Reineker, E. Mena-Osteritz, P. Bäuerle, *J. Lumin.* **2004**, *110*, 225 – 231.
[39] R. J. Cogdell, J. Kohler, *Biochem. J.* **2009**, *422*, 193 – 205.
[40] J. K. Sprafke, D. V. Kondratuk, M. Wykes, A. L. Thompson, M. Hoffmann, R. Drevinskas, W. H. Chen, C. K. Yong, J. Karnbratt, J. E. Bullock, M. Malfois, M. R. Wasielewski, B. Albinsson, L. M. Herz, D. Zigmantas, D. Beljonne, H. L. Anderson, *J. Am. Chem. Soc.* **2011**, *133*, 17262 – 17273.
[41] J. Clark, C. Silva, R. H. Friend, F. C. Spano, *Phys. Rev. Lett.* **2007**, *98*, 206406.
[42] N. J. Hestand, F. C. Spano, *J. Phys. Chem. B* **2014**, *118*, 8352 – 8363.
[43] C. K. Yong, P. Parkinson, D. V. Kondratuk, W. H. Chen, A. Stannard, A. Summerfield, J. K. Sprafke, M. C. O'Sullivan, P. H. Beton, H. L. Anderson, L. M. Herz, *Chem. Sci.* **2015**, *6*, 181 – 189.
[44] J. R. Lakowicz, *Principles of Fluorescence Spectroscopy*, Springer, New York, **2006**.
[45] M. H. Chang, M. Hoffmann, H. L. Anderson, L. M. Herz, *J. Am. Chem. Soc.* **2008**, *130*, 10171 – 10178.
[46] J. C. Phillips, R. Braun, W. Wang, J. Gumbart, E. Tajkhorshid, E. Villa, C. Chipot, R. D. Skeel, L. Kalé, K. Schulten, *J. Comput. Chem.* **2005**, *26*, 1781 – 1802.
[47] J. Lee, V. Stepanenko, J. Yang, H. Yoo, F. Schlosser, D. Bellinger, B. Engels, I. G. Scheblykin, F. Wurthner, D. Kim, *ACS Nano* **2013**, *7*, 5064 – 5076.
[48] G. Rossi, R. R. Chance, R. Silbey, *J. Chem. Phys.* **1989**, *90*, 7594 – 7601.
[49] M. Rumi, G. Zerbi, *Chem. Phys.* **1999**, *242*, 123 – 140.

Received: May 21, 2015
Revised: July 20, 2015
Published online: August 31, 2015

